

Article

Optimization of Radiators, Underfloor and Ceiling Heating towards the Definition of a Reference Ideal Heater for Energy Efficient Buildings

Andrea Ferrantelli ^{1,*}, Karl-Villem Vösa ¹ and Jarek Kurnitski ^{1,2}

¹ Tallinn University of Technology, Department of Civil Engineering and Architecture, Ehitajate tee 5, 19086 Tallinn, Estonia; andrea.ferrantelli@ttu.ee (A.F.); Karl-Villem.Vosa@ttu.ee (K-V.V.)

² Aalto University, Department of Civil Engineering, P.O.Box 12100, 00076 Aalto, Finland; jarek.kurnitski@ttu.ee

* Correspondence: andrea.ferrantelli@ttu.ee; Tel.: +358-404168635

Abstract: Heat emitters constitute the primary devices used in space heating and cover a fundamental role in the energy efficient use of buildings. In the search for an optimized design, heating devices should be compared with a benchmark emitter with maximum heat emission efficiency. However, such an ideal heater still needs to be defined. In this paper we perform an analysis of heat transfer in a European reference room, considering room side effects of thermal radiation and computing the induced operative temperature both analytically and numerically. By means of functional optimization, we analyse trends such as the variation of operative temperature with radiator panel dimensions, finding optimal configurations. In order to make our definitions as general as possible, we address panel radiators, convectors, underfloor (UFH) and ceiling heating. We obtain analytical formulas for the operative temperature induced by panel radiators and identify the 10-type as our ideal radiator, while the UFH provides the best performance overall. Regarding specifically UFH and ceiling heaters, we find optimal sizes that identify the according ideal emitters. The analytical method and quantitative results reported in this paper can be generalized and adopted in most studies concerning the efficiency of different heat emitter types in building enclosures.

Keywords: radiator efficiency; energy; operative temperature; analytical model; computer simulations

1. Introduction

The energy performance of heating emitters is a key factor in the energy demand of the building sector, which is primarily determined by space heating [1–3]. Such devices can be of very different type (panel radiators, convectors, ceiling and underfloor heating...), each determining the energy demand in a specific way [4–8]. For these reasons, several studies have investigated the emitters performance on both the experimental and theoretical viewpoint [9–11], focusing especially on the design, specific type and room placement of panel radiators (e.g. close to a window or slightly detached from a wall) [4,12–18]. For instance, measurements have shown a better performance of low temperature panel radiators [19], and a sensibly different outcome for serial and parallel connected radiators [9].

Despite such recent advances, this kind of investigation seems to be very involved, for a variety of reasons. Contrasting results also exist: an experimental investigation of a convector, a radiant and a baseboard heater showed a lower energy consumption by the convector [7], in contrast with the classic work by Olesen et al. [4], written in the early 80s. While it was concluded in [7] that the cause was probably the improved flow outlet design of the newer convector, an older study already considering this improvement [13] agreed instead with [4].

Another crucial problem is the lack of a staple or ideal emitter, to use as a reference device with maximum efficiency. For air temperature control, an ideal heater is generally described as a dimensionless point heater (Figure 1). Heat is transferred via convection to the thermal node of indoor air and via radiation to the surrounding surfaces. A higher convective transfer fraction induces lower

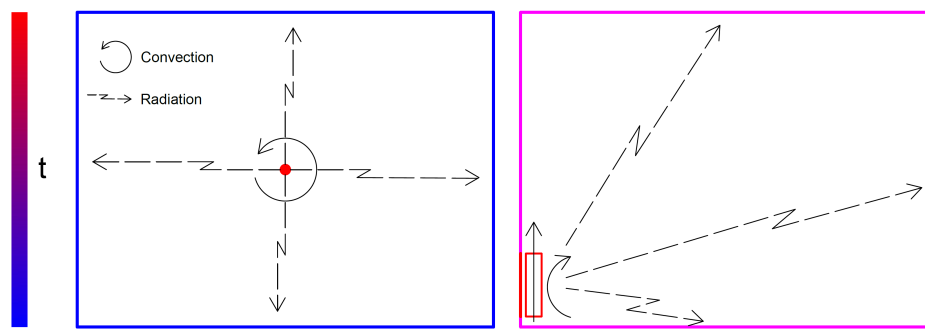


Figure 1. Ideal point heater (left) and real heat emitter (right).

surface temperatures on the surrounding surfaces with minimal heat loss, as in Fig.1. To reach the desired air temperature set-point t_{air} , an emitter with convective fraction of 1 (pure convection) thus requires the lowest possible heat output. In this sense, it represents an "ideal" heater.

Nevertheless, since heating consumption is nowadays assessed in function of thermal comfort, the so-called operative temperature (op.t.) t_{op} is being increasingly used [9,13,18,20]. This is defined as the uniform temperature of an enclosure in which an occupant would exchange the same amount of heat by radiation and convection as in the existing non-uniform environment [21]. By definition, t_{op} is thus proportionally related to the temperature of surrounding surfaces. In this respect, the "ideal" device described above should now exhibit a lower performance, as it heats the surrounding surfaces only minimally. As we will illustrate, preliminary simulations with the software IDA ICE [22] confirm indeed that a number of real emitter configurations can outperform the point heater (convector).

In other words, defining an ideal benchmark heater for operative temperature control is non-trivial, and needs to be addressed for better comparison between different heat emitter systems. To this aim, we consider an average-sized enclosure provided by the CEN technical committee TC130 working group WG13, with a user sitting in the middle (Figure 2). We investigate how the operative temperature changes with the typology and size of emitter, and whether there exist optimal configurations corresponding to the highest t_{op} . We address panel radiators (10- and 21-type), underfloor (UFH) square, UFH strip and ceiling heating.

By computing numerically the steady-state heat transfer in the enclosure with IDA ICE, we obtain surface temperatures for all the walls, for each specific configuration; these values are then used as boundary conditions for an analytical calculation that follows the ISO Standard [21]. The analytical calculation is necessary for two main reasons: first, as we explain in the text, IDA ICE calculates the view factors and accordingly the mean radiant and operative temperatures in a very specific way that is different from the ISO procedure¹. As we are aiming to contribute to the heat emission code EN 15316-2-1:200, it is advisable to use a standard procedure.

Secondly, and more importantly, we are able to extrapolate and generalize our results to *any* emitter size, for each type here considered. This is accomplished with a simple interpolation method which was introduced in [23] when assessing domestic hot water consumption.

For the case of panel radiators, keeping the heat output constant we determine analytical t_{op} curves for both the panel radiators in function of their size. This allows highlighting rigorously several features of panel radiators, such as the existence of an optimal width range for the operative temperature and a qualitative difference in t_{op} variations for the 10- and 21-type. Finally, we find that the 10-type is the most performing and can be regarded as the "ideal" radiator.

Underfloor and ceiling heating show a similar behaviour, with operative temperatures approaching, and often exceeding, the air temperature. Analytical and numerical calculations have an

¹ We will show that the t_{op} obtained this way is not radically different from the analytical result.

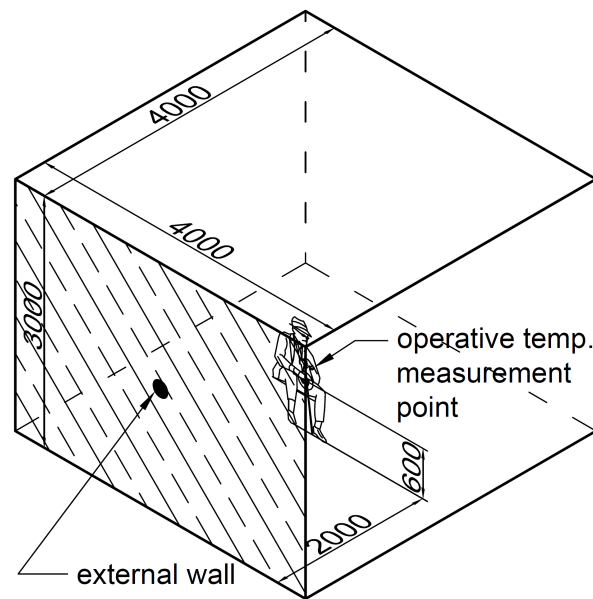


Figure 2. Room setup.

excellent agreement and show a maximum t_{op} for sizes smaller than the whole width of the room. The analytical solution allows to find their location precisely, up to three digits².

Let us remark that our specific predictions are validated by well-tested approaches such as the view factors (see e.g. the standard [21]). Although our specific results, e.g. the location of maximum t_{op} for strip heaters, pertain to a well-defined problem in our configuration (that is, the test room without openings), here we have shown quantitatively two general features: how the radiator performance changes with panel area, and the existence of optimal sizes for UFH and ceiling heating.

Additionally, our analytical study introduces a simple, yet general and predictive method for computing the operative temperature for *any* panel size and radiator type. For the case at hand, we list a series of analytical formulas for calculating t_{op} for radiators of 10- or 21-type, with panel size in the range considered and excluding back wall losses.

The present paper is organized as follows: in Section 2 we describe the test chamber, the simulation setup and the different methods for computing the operative temperature. In Section 3 we report our results for each single case while Section 4 contains a summary of our findings and concluding remarks. In the Appendix we report considerations about the view factors, a comparison between our analytical and numerical methods and the analytical formulas for determining the operative temperature for any radiator size.

2. Method

In this study, we consider an enclosure with thermal layer properties and dimensions 4m×4m×3m specified by the CEN TC130 European Committee, shown in Figure 2. The U-value of external wall is 0.25 W/m²K, and the room was ventilated with heat recovery ventilation providing air change rate of 1 l/h.

As it was shown in [8], gradients measured for radiators and UFH were approximately 0 K/m for ventilated rooms. We accordingly neglected the vertical temperature gradient. This approximation is therefore true at least for radiators and UFH, however no information exists for ceiling heating.

² In theory one might conclude that the UFH is the ideal heater, but in practical cases the embedded emission losses are relevant [8].

We locate the calculation point, namely the centre of mass of an average sitting user, at 0.6m above the floor in the room centre (i.e., at 2m distance from each wall) [21]. The most performing heater configuration will then be the one for which the operative temperature is maximal, with the same heater nominal output. The steady-state boundary conditions are the following: Indoor air temperature $T_{in}=20\text{ }^{\circ}\text{C}$, external air temperature $T_{ext}=-15\text{ }^{\circ}\text{C}$, external relative humidity $RH=85\%$. Both direct normal and diffuse horizontal irradiance are set to zero.

The operative temperature t_{op} is computed analytically, according to the prescriptions of the ISO 7726 standard, as we explain in the following. Considering the contributions of all the six surfaces in the enclosure, we obtain an expression for $t_{op} = t_{op}(a, b)$ that is a function of the radiator height a and width b . The eventual global maxima of this function in the (a, b) plane would then correspond to the optimal configuration for that specific heater. Such full analytical solution is then numerically validated by the finite difference method software IDA ICE [22] in the same CEN TC130 test room, in the limit when only the contribution of the surfaces that are parallel to the principal calculation surface is accounted for.

The operative temperature at the above location is not uniquely defined. In IDA ICE it is evaluated as the simple arithmetic average of air temperature t_{air} and the mean radiant temperature \bar{t}_r [22],

$$t_{op} = \frac{t_{air} + \bar{t}_r}{2}, \quad (1)$$

(throughout this paper, $[t_i]=[\text{ }^{\circ}\text{C}]$ and $[T_i]=[\text{K}]$). This differs from the exact definition given in the ISO 7726 [21],

$$t_{op} = \frac{h_c t_{air} + h_r \bar{t}_r}{h_c + h_r} \equiv A t_{air} + (1 - A) \bar{t}_r, \quad (2)$$

where the average is weighted by the radiation and convection heat transfer coefficients h_r and h_c at the calculation point³. Here t_{air} is the air temperature and \bar{t}_r the mean radiant temperature. The explicit formula for the coefficient A , which is itself a function of h_c and h_r , is given in the Appendix; for our setup, it lies within the range $A \sim 0.5 - 0.6$.

Another difference between the ISO standard and IDA ICE is that the numerical software has a peculiar way of computing the mean radiant temperature \bar{t}_r . It considers only the surfaces that are *parallel* to the principal calculation surface, therefore the sum of view factors in a principal direction is < 1 (Figure 3). Moreover, \bar{t}_r is obtained as the average of mean radiant temperatures from the six principal directions, weighted by the respective view factors,

$$\bar{T}_{mrt} = \sqrt[4]{\frac{\sum_{i=1}^6 \sum_{j=1}^n F_{i \rightarrow j} T_j^4}{\sum_{i=1}^6 \sum_{j=1}^n F_{i \rightarrow j}}}, \quad (3)$$

where the $F_{i \rightarrow j}$ are computed for a small area (the observer) that is only parallel to the radiating surface.

In contrast, the ISO 7726 prescribes that for each direction one considers both *parallel and perpendicular* surfaces (see Figure 4), obtaining the plane radiant temperature [14,21],

$$\bar{T}_{pr}^{(i)} = \sqrt[4]{\sum_{j=1}^6 F_{p-A_j} T_{sj}^{(i)4}}, \quad (4)$$

³ As we demonstrate in the Appendix, in reality the different operative temperature values which are obtained with either method show no sizeable qualitative difference.

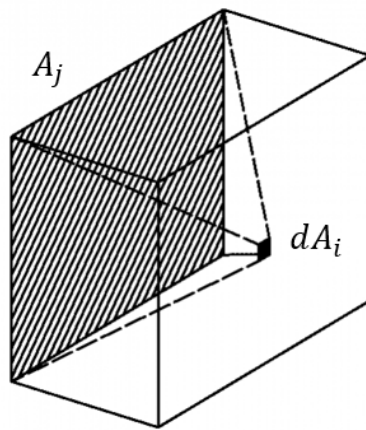


Figure 3. Calculation of mean radiant temperature from IDA-ICE [22].

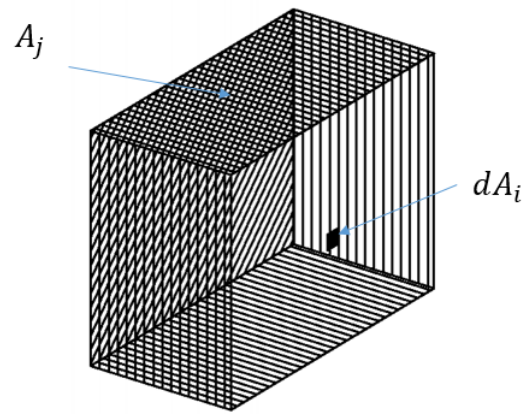


Figure 4. Calculation of mean radiant temperature from ISO 7726 [21].

with the angle factors F_{p-A_j} as given in the Appendix. Now the sum of view factors in each direction is accordingly =1, and the mean radiant temperature is given by [21],

$$\bar{t}_r(a, b, c) = \sqrt[4]{\frac{\sum_{i=1}^6 \beta_i \bar{T}_{pr}^{(i)}(a, b, c)}{\sum_{i=1}^6 \beta_i}} - 273.15, \quad (5)$$

namely by a weighted average over the projected area factors β_i of a person, listed in Table 1.

Table 1. Projected area factors of a person [21].

	Standing	Seated
Up/down	0.08	0.18
Left/right	0.23	0.22
Front/back	0.35	0.30

Specifically, in this work all the "Analytical Full" t_{op} points in the graphs are calculated with Eqs.(2) and (5), therefore following the ISO standard completely throughout this paper. The only point in common with IDA ICE consists of the surface temperatures $T_{sj}^{(i)}$, which are written as polynomial interpolations from the data provided by the software. Since both the definitions of operative and mean radiant T are different, the analytical t_{op} is independent of the numerical t_{op} .

On the other hand, for the "Analytical as IDA ICE" points, while still computing analytically, we use Eqs.(1) and (3), consistently with the software. This provides validation of both our view factors and the temperature interpolations $T_{sj}^{(i)} = T_{sj}^{(i)}(x)$, where x is a length that is specific to the particular case (either a or b). The interpolations are implemented towards a more general form of the operative temperature than by using the raw data for the surface temperatures. This way, instead of calculating t_{op} for each point, we can write $t_{op} = t_{op}(x)$ and accordingly formulate general considerations and predictions on the operative temperature for *any* possible configuration consistent with the test room setup. In the case of UFH and ceiling heating, the "square" configuration consists of a square heater placed under the floor or ceiling surface, centred in the middle of the room, where the user is sitting. The "strip" configuration instead considers a heated strip running from the cold (or external) wall. Further descriptions are given in Sections 3.2 and 3.3.

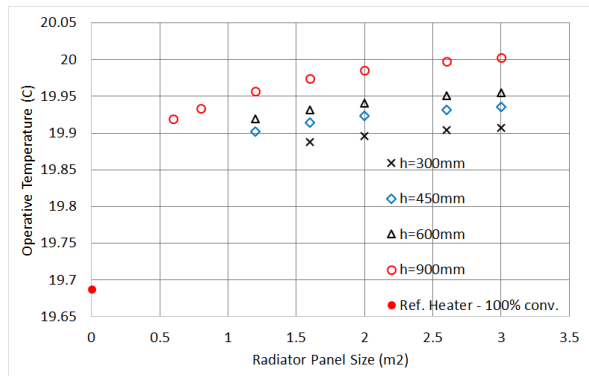


Figure 5. IDA ICE operative temperatures for a 10-type radiator and convector in function of the panel area.

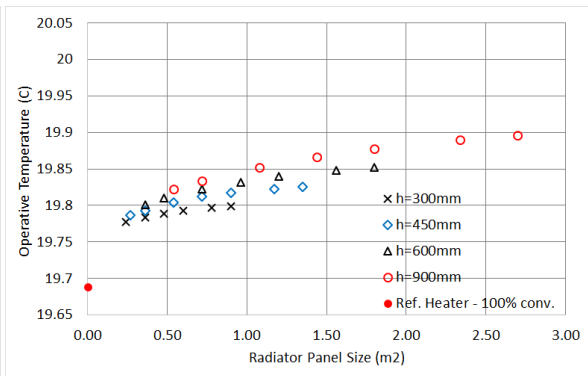


Figure 6. IDA ICE operative temperatures for a 21-type radiator and convector in function of the panel area.

3. Results and Discussion

3.1. Panel radiator

As discussed in the previous section, in this study we consider a room with a single external wall and adiabatic internal walls, floor and ceiling under steady-state conditions. Thermal layer properties and room dimensions (Figure 2) are chosen according to the CEN TC130 European Committee specification, namely the U-value of external wall is 0.25 W/m².K. Different types and sizes of heat emitters (radiators, UFH and ceiling heater) are used in IDA ICE simulations to offset the heat loss through the external wall (details specific to a type of emitter are presented in their relevant sections). The resulting surface temperatures as calculated by the software are logged and used as input in the analytical calculation. Operative temperatures computed by IDA ICE are also used for comparison with the analytical result.

Figures 5 and 6 illustrate first of all that the area by itself is not a good parameter for assessing the performance: given the same area, the efficiency varies with height. Additionally, and more importantly, we observe that one cannot identify a reference ideal convector with 100% convection and 0% radiation as an ideal heater, since it returns the lowest operative temperature.

Operative temperatures for fixed heights are plotted in Figures 7 and 8. These hold respectively for a 10-type and a 21-type panel radiator (some values for the 10-type are missing, as it could not reach 134W of power output). One can see that in general, the numerical and analytical solutions are nearly equivalent. Only for the 10-type we see a slight deviation; moreover, the 10-type reveals to be the most performing heater, with t_{op} values always exceeding those of the 21-type by $\sim 0.1^{\circ}\text{C}$. They can even approach the air temperature 20°C at $h = 0.9\text{m}$. We can thus conclude that for the study at hand the 10-type can be identified as our "ideal" radiator.

Further conclusions can be made rigorous by means of our analytical solution. First of all, the t_{op} values are linearly distributed along different heights h . By applying a method first introduced in [23], we interpolate the operative temperature versus the height (minimum square method), for a fixed width. The according curves can be generally written as

$$t_{op}(h, w) = A(w)h + B(w), \quad (6)$$

returning the operative temperature in the range $0.3\text{m} \leq h \leq 0.9\text{m}$, for any desired height h , by using the explicit formulas listed in Tables A1 and A2.

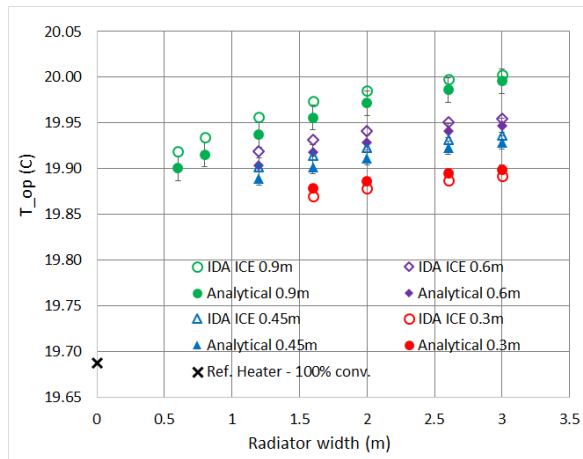


Figure 7. Operative temperatures for a 10-type panel radiator, with $h = 0.3, 0.45, 0.6, 0.9\text{m}$.

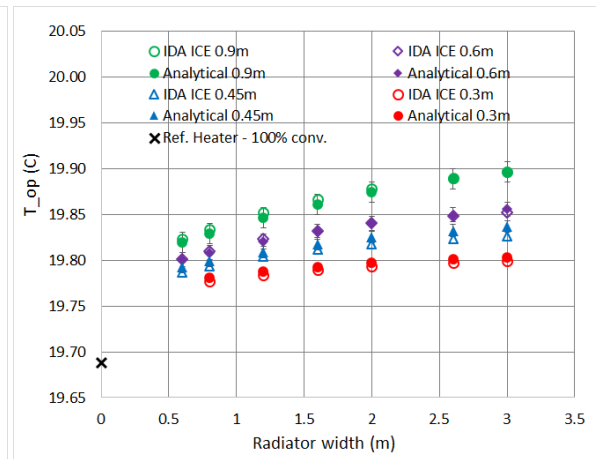


Figure 8. Operative temperatures for a 21-type panel radiator, with $h = 0.3, 0.45, 0.6, 0.9\text{m}$.

In contrast, we can show that, assuming a given height, the t_{op} values are *not* linearly distributed along different widths w , rather they follow a quadratic law

$$t_{op}(h, w) = A(h)w^2 + B(h)w + C(h). \quad (7)$$

As it is shown in Tables A3 and A4, one finds $A(h) < 0$ for any height. t_{op} grows instead linearly with increasing width, because $A(w) > 0$: this verifies the physical result that the operative temperature is more dependent on the height than on the width⁴.

The analytical solution allows to make even more specific conclusions. As an example, consider the 21-type radiator. The explicit form of the operative temperature is generally highly non linear, however plotting the first derivative $Dt_{op} \equiv dt_{op}/dw$ in function of the width returns additional information. In Figure 9 we find indeed a "plateau" starting at $w \sim 1\text{m}$ and ending at about 2m , where the decrease with w is less pronounced: in other words, in the according range Δw the operative temperature t_{op} is optimised with respect to width increase, and widths contained in this interval are most advantageous.

The approximated range Δw above is probably precise enough for practical applications, however an analytical formula such as Eq.(7) allows to identify its boundaries with high precision. The second and third derivatives $D^2t_{op} \equiv d^2t_{op}/dw^2$ and $D^3t_{op} \equiv d^3t_{op}/dw^3$ provide indeed the exact locations of the plateau, at $w = 0.87\text{m}$ and $w = 1.86\text{m}$ respectively. The latter point corresponds to a minimum of D^3t_{op} , which identifies a change of concavity in D^2t_{op} . Finally, the second derivative gives the exact point of minimal increment of t_{op} , sitting at $w = 2.736\text{m}$. Interestingly, exactly the same value holds for $h = 0.9\text{m}$, as shown in Figure 10.

To summarize, investigating the performance of 10- and 21-type panel radiators we have found rigorously that

- given the same area, the efficiency varies with height,
- an ideal convector with 100% convection performs worse than panel radiators,
- the 10-type can be identified as our ideal heater,
- the operative temperature is more dependent on the height than on the width,
- there exists an ideal width range for 21-type radiators.

⁴ One can also prove that Eqs.(6) and (7) are equivalent, namely by substituting one value for h and w they return the same t_{op} (discrepancy of order ~ 0.001 , around 0.02%).

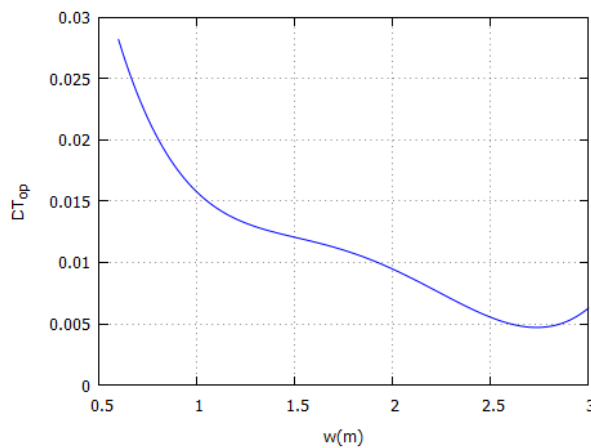


Figure 9. First derivative of the analytical operative temperature for a 21-type radiator, $h = 0.3\text{m}$.

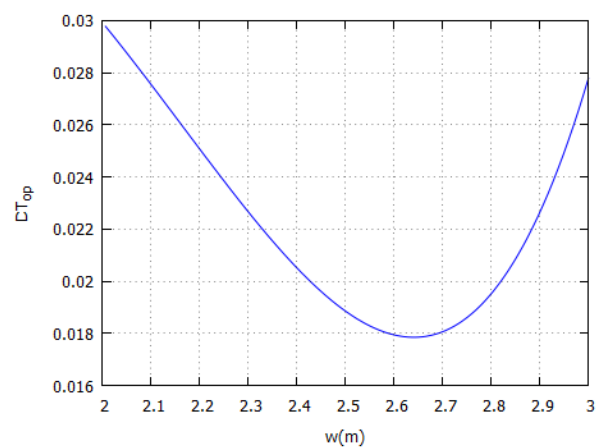


Figure 10. First derivative of the analytical operative temperature for a 21-type radiator, $h = 0.9\text{m}$.

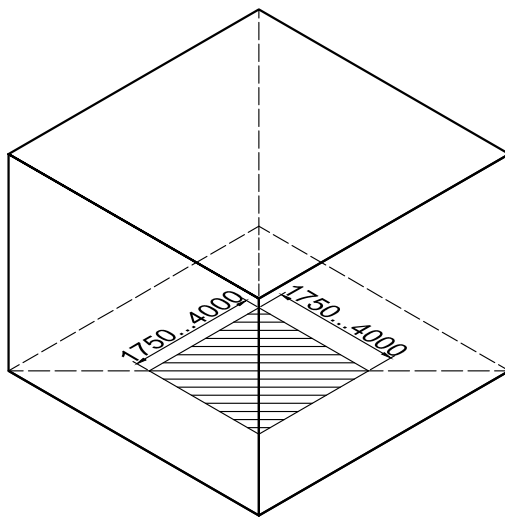


Figure 11. Underfloor heating - square setup

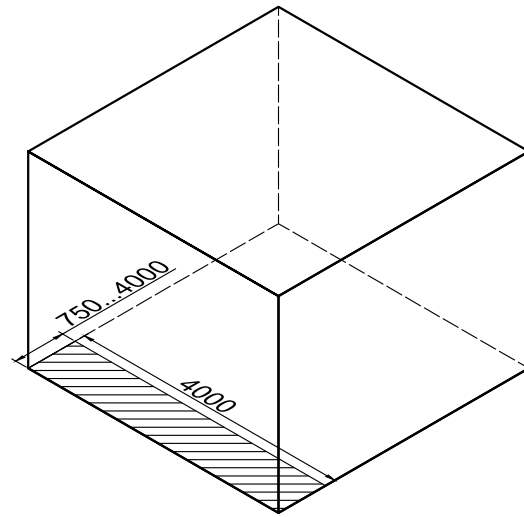


Figure 12. Underfloor heating - strip setup

Furthermore, we provide in Tables [A1](#) to [A4](#) useful analytical formulas which determine precisely the operative temperatures for any width and height in the ranges considered in the study at hand.

3.2. Underfloor heating

Regarding underfloor heating (UFH), we considered two different setup: a square one in the centre of the floor, with varying side length (Figure 11), and a strip setup with room width and varying depth from the external wall (Figure 12). Nominal heat output of 50 W/m^2 at a water-side temperature drop of $\Delta T = 7\text{K}$ was used as input for the IDA ICE model, with the piping at a depth of 25mm in screed. Supply temperature of 35°C was used. The operative temperature for square and strip UFH is plotted in Figs. 13 and 14 respectively. Here we compare IDA ICE (dots) with an analogous analytical calculation with no projection on perpendicular surfaces (crosses) and with the full analytical calculation (all the 6 directions with perpendicular surfaces), diamonds.

In both cases the analytical model agrees with the numerical computation with an excellent precision. Notice however how the full solution deviates by $\sim 0.1^\circ\text{C}$ from IDA ICE unless the square width is around 2m : considering the horizontal and vertical walls as a whole, this case corresponds to the most symmetric configuration indeed. As it can be seen by investigating the view factors of each

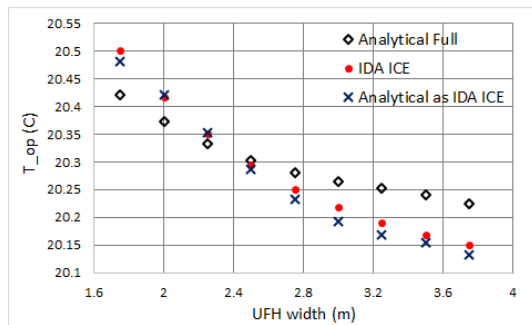


Figure 13. Operative temperature for a square UFH.

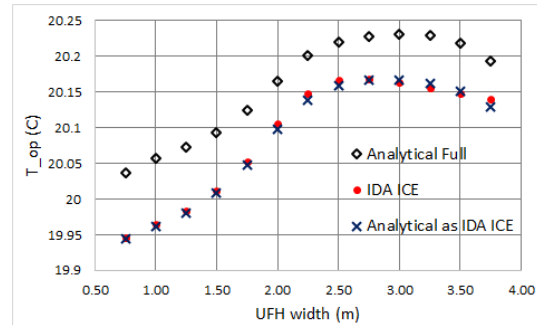


Figure 14. Operative temperature for a strip UFH.

surface, for smaller squares $w < 2\text{m}$ IDA ICE does not account for the heat dissipation to the vertical walls⁵. On the other hand, for $w > 2\text{m}$ these contribute to increasing t_{op} at the calculation point (2m from each wall, at 0.6m from the floor). The main result in any case is that there is no evident optimal size for the UFH with this configuration.

In the case of UFH as a strip running between the side walls, starting from the cold wall, we find instead something more interesting. Neglecting the vertical walls we get again an excellent cross-check with IDA ICE; furthermore, the extension to the full enclosure shows a systematic difference of nearly 0.1°C , accounting for the effect of vertical walls. While qualitatively there is basically no deviation with the numerical solution, this is interesting when considering precision calculations.

More importantly, we find a very distinct maximum for t_{op} between 3m and 3.1m, Figure 14. By means of the analytical form of the solution, we can compute its location precisely at $w = 3.0372\text{m}$, see Fig.19. Notice also that the operative temperature difference between radiators and a 3.75m large UFH is consistent with the experimental paper [8], where this was computed to be 0.28K .

3.3. Ceiling heating

The two configurations of square and strip heaters we addressed for floor heating were also considered for the ceiling (Figures 15 and 16). Geometrically, the setup is basically a mirror-reflection of the floor model on the vertical axis. The main difference in the view factors is in the calculation point, which now sits at 2.4m from the heated surface, making the reflection not perfectly symmetrical. Catalogue values of a well-known manufacturer were applied for the IDA ICE model input (nominal heat output of 591.7 W/m^2 at $\Delta T_{in} = 50\text{K}$ with characteristic exponent $n=1.174$). Supply temperature of 45°C was used. The operative temperatures in this case are given in Figures 17 and 18, and the absolute maximum for a heated strip is shown in Fig.20. It occurs at $x = 3.1349\text{m}$.

Comparing Figure 17 with Fig.13, we notice a marginal difference for $w < 2\text{m}$, while otherwise the same larger t_{op} with respect to IDA ICE is obtained. The operative temperature values are naturally smaller in this case, due to the larger distance heater - observer that reduces the heat transfer. For a heated strip, this is reflected in Figure 18, showing a smaller effect of the vertical walls in comparison to Figure 14. Qualitative differences are irrelevant.

4. Conclusions

Thermal comfort is strictly related to the energy efficiency of heating systems in buildings, and it can be quantified by the operative temperature t_{op} , namely the temperature sensed by the user. In this paper we performed a rigorous investigation of the operative temperature induced on users by several types of different heat emitters, in the search for the most performing, or ideal, heater. We

⁵ These lower values hold also if one uses the IDA ICE data directly, therefore they are not due to errors related to the interpolations of the surface temperatures.

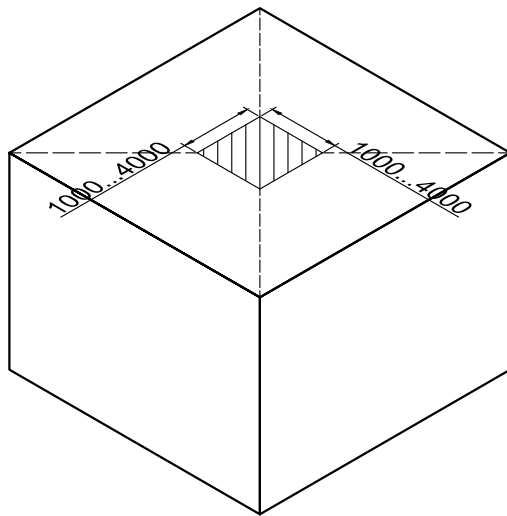


Figure 15. Ceiling panel - square setup

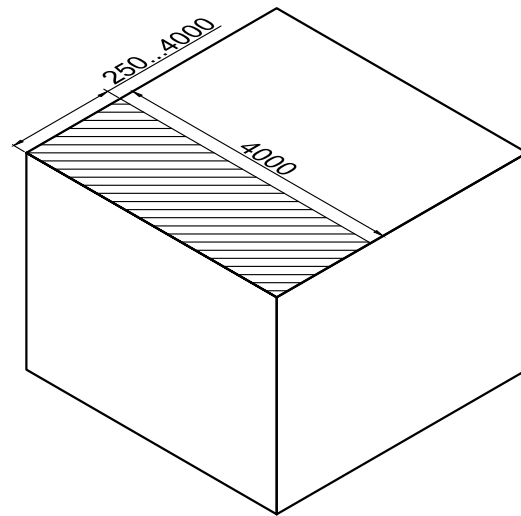


Figure 16. Ceiling panel - strip setup

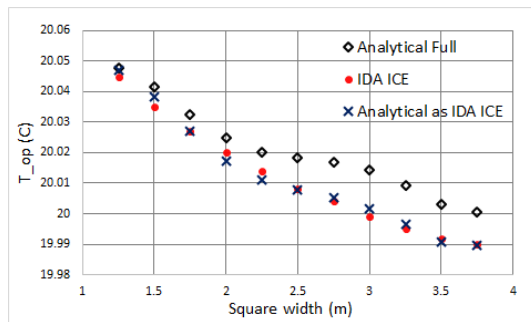


Figure 17. Operative temperature for a heated square portion of the ceiling.

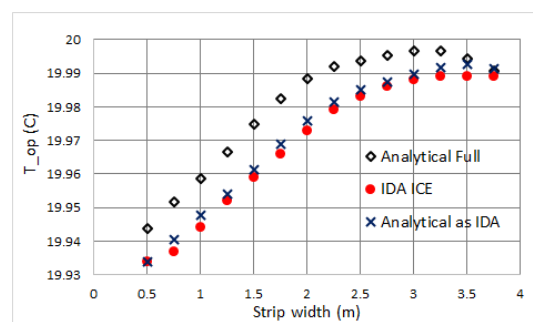


Figure 18. Operative temperature for a heated strip on the ceiling.

considered a number of configurations of practical interest, with analytical and numerical calculations of t_{op} performed in a test room with a standard size.

Specifically, considering panel radiators and underfloor and ceiling heaters, we obtained the overall behaviour of operative temperature as a function of emitter type, size and room geometry. We addressed panel radiators of 10- and 21-type installed on the cold wall, for a variety of sizes and surface temperatures. Compared with an ideal convector providing the same output $\sim 134W$, we found the 10-type is the most performing. For larger sizes, the 10-type radiator is even capable to induce an operative temperature that is equal to the air temperature $20^{\circ}C$. This means that it constitutes our "ideal" radiator for the setup at hand.

Via our analytical calculations we were able to draw a number of considerations, proving for instance that the performance of radiators is more sensitive to the height than to the width, and providing according exact formulas. These can be of practical use for radiators of 10- or 21-type with dimensions $0.3m \leq h \leq 0.9m$ and $1.2m \leq w \leq 3m$, assuming no back wall losses; they are listed in Tables A1 to A4. Furthermore, in the case of 21-type panel radiators we also highlighted a width interval for which adopting larger panels is most convenient, as it contains a size range that optimizes the operative temperature.

For underfloor UFH and ceiling heating strips, we identified the occurrence of non-trivial global maxima, corresponding to the highest temperature sensed by a person sitting in the middle of the room. Also, via the systematic difference between numerical and analytical values shown in our plots, one could quantify precisely the effect of the vertical walls, which are ignored in the numerical calculation. The difference, though rather small, is however sizeable.

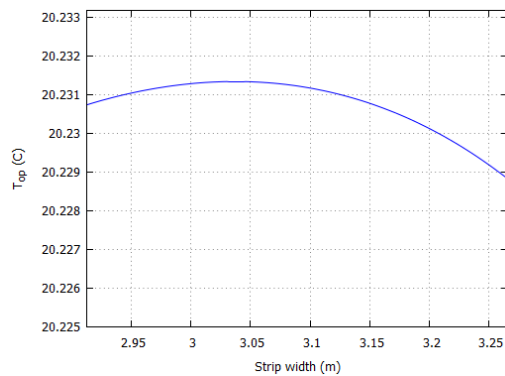


Figure 19. Operative temperature maximum for a strip heated area underfloor.

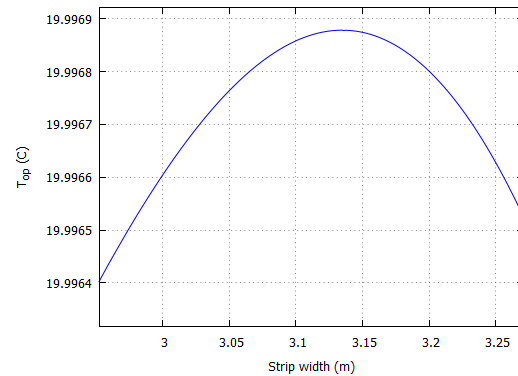


Figure 20. Operative temperature maximum for a heated strip on the ceiling.

We notice that the ceiling heating t_{op} is very close to the 10-type radiator, and that the UHF optimal strip measuring 3/4 of the room width may correspond to our overall ideal heater, since it provides a 0.23 K higher op.temp. than the 10-type radiator⁶. Furthermore, compared to typical radiator sizes with height 0.6m, the UFH provides 0.25 K - 0.3 K higher t_{op} relative to the 10-type and 0.35 K relative to the 21-type.

The fact that the op.temp. approaches the air temperature is very advantageous for energy saving, as it was shown e.g. in [24] that the energy demand is very sensitive to operative temperature corrections. In particular, a difference of only 0.1°C is capable of inducing an increase of the annual heating need by 1-2% [24]: such effect is found for the convector and 21-type panel radiator, which are therefore fairly underperforming. Specifically, the former shows the worst performance: the op.temp. is by 0.55 K lower compared to UFH. However, the air and operative temperature differences calculated in this study should not be directly applied for energy saving assessment, because they are valid at the outdoor temperature -15°C, which is much lower than the average heating season value.

The investigation presented in this paper constitutes a good starting point for a number of improvements in the search for an ideal heater. First of all, parametric studies on the relationship between view factors, room and geometry of the emitter might show a more general pattern, whose impact on the whole energy demand could be quantified with e.g. annual simulations.

Funding: The research was supported by the Estonian Research Council with Institutional research funding grant IUT1-15. The authors are also grateful to the Estonian Centre of Excellence in Zero Energy and Resource Efficient Smart Buildings and Districts, ZEBE, grant 2014-2020.4.01.15-0016 funded by the European Regional Development Fund.

Conflicts of Interest: The authors declare no conflict of interest.

Appendix View factors and operative temperature formulas

The view factors for a small area parallel or perpendicular to a surface of height a and width b , separated by a distance c , hold respectively as [21]

$$F_{p-A_i} = \frac{1}{2\pi} \left(\frac{X}{\sqrt{1+X^2}} \arctan \frac{Y}{\sqrt{1+X^2}} + (X \leftrightarrow Y) \right), \quad (A1)$$

⁶ Clearly, though the UFH and ceiling smallest squares provided the highest operative temperature, such cases should rather be considered as not realistic, because the small square heater should track the occupants when they move around the room.

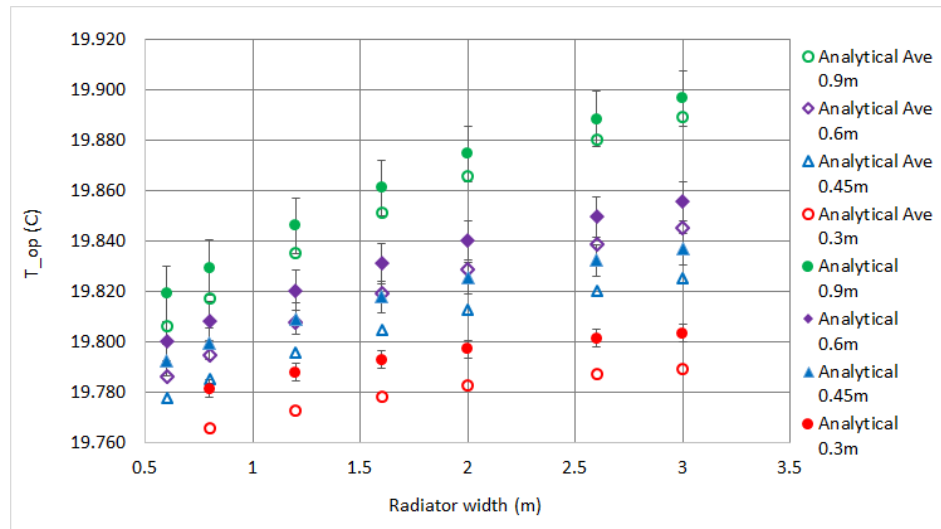


Figure A1. Operative temperatures for a 21-type panel radiator, arithmetic average vs average weighted with convection.

with $X = a/c$, $Y = b/c$, and

$$F_{p-A_i} = \frac{1}{2\pi} \left(\arctan \frac{1}{Y} - \frac{Y}{\sqrt{X^2 + Y^2}} \arctan \frac{1}{\sqrt{X^2 + Y^2}} \right), \quad (\text{A2})$$

with $X = a/b$, $Y = c/b$. We should remark that the calculation of mean radiant temperatures for the perpendicular surfaces is extremely sensitive to how the above view factors are implemented. For example, in Section 3.1 we discussed panel radiators of varying height h that are installed on the cold wall, at 15cm from the floor. In this case, one could naively compute the view factor from the lower edge of the cold wall up to the top of the radiator ($a = h + 15\text{cm}$), or alternatively ignoring the 15cm displacement ($a = h$). It can be shown that the view factor differs critically for both cases and returns a non physical result for the operative temperature.

The reason is that the above functions are not linear in a, b, c : since the view factors are additive, a more correct way to calculate them with formulas (A1) and (A2) consists of subtracting F_{p-A_i} at $a = h$ from F_{p-A_i} at $a = h + 15\text{cm}$. This way one obtains a *net* view factor, which despite not being 100% accurate, returns physical operative temperatures that match earlier results [20,24] and the present numerical simulations (see e.g. Figs. 17 and 18).

We conclude with a few considerations about the definition of operative temperature adopted in this paper. In Section 2 we remarked that IDA ICE uses the simple arithmetic average of air temperature t_{air} and mean radiant temperature \bar{t}_r , Eq.(1). On the other hand, for the analytical calculation we used the exact formula for computing the op.t., Eq.(2). The A coefficient is expanded as

$$A \equiv \left(1 + \frac{h_r}{h_c} \right)^{-1}, \quad (\text{A3})$$

and we expand h_c and h_r explicitly in function of the air and mean radiant temperatures by means of the following [14],

$$h_c = 2.38 \sqrt[4]{t_{cl} - t_{air}}, \quad (\text{A4})$$

if $2.38 \sqrt[4]{t_{cl} - t_{air}} > 12.1 \sqrt{V_{air}}$, otherwise

$$h_c = 12.1 \sqrt{V_{air}}, \quad (\text{A5})$$

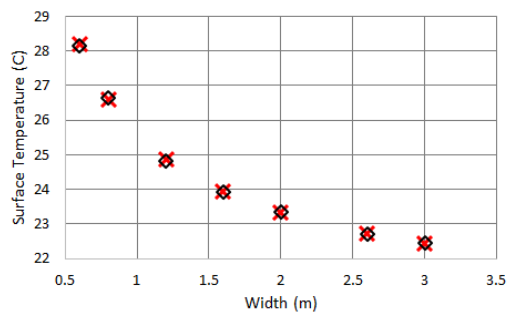


Figure A2. Comparison of surface temperatures for a 21-type radiator, $h = 0.9\text{m}$. IDA ICE (crosses) vs 4th order polynomial interpolation (diamonds).

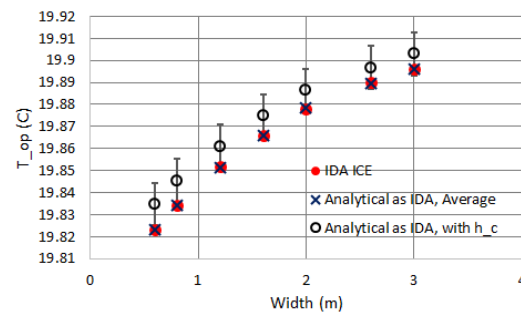


Figure A3. Operative temperatures for a 21-type panel radiator, IDA ICE cross-check: arithmetic average vs weighted average.

with V_{air} the air velocity relative to the human body. The heat transfer coefficient for radiation holds instead as

$$h_r = \sigma \epsilon_{cl} \frac{A_r}{A_D} \frac{(t_{cl} + 273.15)^4 - (\bar{t}_r + 273.15)^4}{t_{cl} - \bar{t}_r}. \quad (\text{A6})$$

Here ϵ_{cl} is the emissivity of a clothed person and A_r/A_D the ratio of the body radiation area (0.67 for crouching, 0.7 for sitting and 0.73 for standing). $\epsilon = 5.67 \times 10^{-8} \text{W}/(\text{K}^4 \text{m}^2)$ is the Stefan-Boltzmann constant. The operative temperature evaluated (ideally) on the surface of a clothed user is thus a function of air and mean radiant temperatures, and of the heat transfer coefficients measured at that same point. As $\bar{t}_r = \bar{t}_r(a, b, c)$, also the radiation coefficient h_r in (A6) is a function of the radiator dimensions a and b , together with the distance radiator-person c .

Comparison of the operative temperature as computed with (2) instead of the arithmetic average (1) is illustrated in Fig.A1. One can see that the difference is not negligible, though the qualitative considerations remain unchanged. It can be easily verified that for underfloor and ceiling heating instead there is a very negligible difference in t_{op} (of the order $\sim 0.01^\circ\text{C}$). Figure A2 also shows the precision of the interpolations used in this paper for a type-21 panel radiator.

One might also wonder about the effect of (2) on the cross-check with IDA ICE, namely when computing the mean radiant temperature without considering the heater projections on the perpendicular surfaces. The result is given in Figure A3.

Quite interestingly, as a last remark, we note that by shifting the point for the calculation of view factors on the surfaces perpendicular to the radiator, one can cancel their effect and recover the IDA ICE result with accuracy close to ~ 0.01 . This curious coincidence perhaps recalls to mind the role of inertial observers in Newtonian mechanics.

Ideal heater APPLIEDSCIENCES

1. Serrano, S.; Ürge Vorsatz, D.; Barreneche, C.; Palacios, A.; Cabeza, L.F. Heating and cooling energy trends and drivers in Europe. *Energy* **2017**, *119*, 425 – 434. doi:https://doi.org/10.1016/j.energy.2016.12.080.
2. D'Agostino, D.; Cuniberti, B.; Bertoldi, P. Data on European non-residential buildings. *Data in Brief* **2017**, *14*, 759 – 762. doi:https://doi.org/10.1016/j.dib.2017.08.043.
3. Yao, R.; Steemers, K. A method of formulating energy load profile for domestic buildings in the UK. *Energy and Buildings* **2005**, *37*, 663 – 671. doi:http://dx.doi.org/10.1016/j.enbuild.2004.09.007.
4. Olesen, B.W.; Mortensen, E.; Thorshaug, J.; Berg-Munch, B. Thermal comfort in a room heated by different methods. *ASHRAE transactions* **1980**, *86*, 34–48.
5. Inard, C.; Meslem, A.; Depecker, P. Energy consumption and thermal comfort in dwelling-cells: A zonal-model approach. *Building and Environment* **1998**, *33*, 279 – 291. doi:https://doi.org/10.1016/S0360-1323(97)00074-7.

6. Olesen, B.W.; de Carli, M. Calculation of the yearly energy performance of heating systems based on the European Building Energy Directive and related CEN standards. *Energy and Buildings* **2011**, *43*, 1040 – 1050. Tackling building energy consumption challenges - Special Issue of ISHVAC 2009, Nanjing, China, doi:https://doi.org/10.1016/j.enbuild.2010.10.009.
7. Léger, J.; Rousse, D.R.; Borgne, K.L.; Lassue, S. Comparing electric heating systems at equal thermal comfort: An experimental investigation. *Building and Environment* **2018**, *128*, 161 – 169. doi:https://doi.org/10.1016/j.buildenv.2017.11.035.
8. Maivel, M.; Ferrantelli, A.; Kurnitski, J. Experimental determination of radiator, underfloor and air heating emission losses due to stratification and operative temperature variations. *Energy and Buildings* **2018**, *166*, 220 – 228. doi:https://doi.org/10.1016/j.enbuild.2018.01.061.
9. Vösa, K.V.; Ferrantelli, A.; Kull, T.M.; Kurnitski, J. Experimental analysis of emission efficiency of parallel and serial connected radiators in EN442 test chamber. *Applied Thermal Engineering* **2018**, *132*, 531 – 544. doi:https://doi.org/10.1016/j.applthermaleng.2017.12.109.
10. Myhren, J.A.; Holmberg, S. Performance evaluation of ventilation radiators. *Applied Thermal Engineering* **2013**, *51*, 315 – 324. doi:https://doi.org/10.1016/j.applthermaleng.2012.08.030.
11. Risberg, D.; Risberg, M.; Westerlund, L. CFD modelling of radiators in buildings with user-defined wall functions. *Applied Thermal Engineering* **2016**, *94*, 266 – 273. doi:https://doi.org/10.1016/j.applthermaleng.2015.10.134.
12. Hasan, A.; Kurnitski, J.; Jokiranta, K. A combined low temperature water heating system consisting of radiators and floor heating. *Energy and Buildings* **2009**, *41*, 470 – 479. doi:https://doi.org/10.1016/j.enbuild.2008.11.016.
13. Ali, A.H.H.; Gaber Morsy, M. Energy efficiency and indoor thermal perception: a comparative study between radiant panel and portable convective heaters. *Energy Efficiency* **2010**, *3*, 283–301. doi:10.1007/s12053-010-9077-3.
14. Kalmár, F.; Kalmár, T. Interrelation between mean radiant temperature and room geometry. *Energy and Buildings* **2012**, *55*, 414 – 421. doi:https://doi.org/10.1016/j.enbuild.2012.08.025.
15. Shati, A.; Blakey, S.; Beck, S. The effect of surface roughness and emissivity on radiator output. *Energy and Buildings* **2011**, *43*, 400 – 406. doi:https://doi.org/10.1016/j.enbuild.2010.10.002.
16. Munaretto, F.; Recht, T.; Schalbart, P.; Peuportier, B. Empirical validation of different internal superficial heat transfer models on a full-scale passive house. *Journal of Building Performance Simulation* **2017**, *0*, 1–22. doi:10.1080/19401493.2017.1331376.
17. Sevilgen, G.; Kilic, M. Numerical analysis of air flow, heat transfer, moisture transport and thermal comfort in a room heated by two-panel radiators. *Energy and Buildings* **2011**, *43*, 137 – 146. doi:https://doi.org/10.1016/j.enbuild.2010.08.034.
18. Jahanbin, A.; Zanchini, E. Effects of position and temperature-gradient direction on the performance of a thin plane radiator. *Applied Thermal Engineering* **2016**, *105*, 467 – 473. doi:https://doi.org/10.1016/j.applthermaleng.2016.03.018.
19. Maivel, M.; Kurnitski, J. Low temperature radiator heating distribution and emission efficiency in residential buildings. *Energy and Buildings* **2014**, *69*, 224 – 236. doi:https://doi.org/10.1016/j.enbuild.2013.10.030.
20. Maivel, M.; Konzelmann, M.; Kurnitski, J. Energy performance of radiators with parallel and serial connected panels. *Energy and Buildings* **2015**, *86*, 745 – 753. doi:https://doi.org/10.1016/j.enbuild.2014.10.007.
21. ISO 7726:1998. Ergonomics of the thermal environment - Instruments for measuring physical quantities. Standard, International Organization for Standardization, 1998.
22. EQUA. IDA ICE - Indoor Climate and Energy. Technical report, EQUA, Stockholm, Sweden, 2013.
23. Ferrantelli, A.; Ahmed, K.; Pylsy, P.; Kurnitski, J. Analytical modelling and prediction formulas for domestic hot water consumption in residential Finnish apartments. *Energy and Buildings* **2017**, *143*, 53 – 60. doi:https://doi.org/10.1016/j.enbuild.2017.03.021.
24. Maivel, M.; Kurnitski, J. Radiator and floor heating operative temperature and temperature variation corrections for EN 15316-2 heat emission standard. *Energy and Buildings* **2015**, *99*, 204 – 213. doi:https://doi.org/10.1016/j.enbuild.2015.04.021.

Table A1. Operative temperature t_{op} (°C) in function of panel width and height, 10-type.

Height (m)	0.30	$-0.0046w^2 + 0.0357w + 19.833$
	0.45	$-0.0066w^2 + 0.0494w + 19.839$
	0.60	$-0.0069w^2 + 0.053w + 19.851$
	0.90	$-0.0111w^2 + 0.0786w + 19.859$
Width (m)	0.60	-
	0.80	-
	1.20	$0.1079h + 19.84$
	1.60	$0.1268h + 19.842$
	2.00	$0.1404h + 19.846$
	2.60	$0.1489h + 19.853$
	3.00	$0.1403h + 19.86$

Table A2. Operative temperature t_{op} (°C) in function of panel width and height, 21-type.

Height (m)	0.30	$-0.0031w^2 + 0.0216w + 19.766$
	0.45	$-0.0049w^2 + 0.0355w + 19.773$
	0.60	$-0.0054w^2 + 0.042w + 19.778$
	0.90	$-0.007w^2 + 0.0573w + 19.788$
Width (m)	0.60	$0.0593h + 19.765$
	0.80	$0.0773h + 19.761$
	1.20	$0.0938h + 19.763$
	1.60	$0.1101h + 19.764$
	2.00	$0.125h + 19.764$
	2.60	$0.1408h + 19.764$
	3.00	$0.1509h + 19.763$

Table A3. Formulas for the coefficients in (6) and (7), 10-type.

A(h)	$-0.1074h^3 + 0.1828h^2 - 0.1045h + 0.0132$
B(h)	$0.6012h^3 - 1.0361h^2 + 0.6114h - 0.0707$
C(h)	19.846
A(w)	$-0.0234w^2 + 0.1174w + 3 \times 10^{-5}$
B(w)	$0.0039w^2 - 0.0054w + 19.841$

Table A4. Formulas for the coefficients in (6) and (7), 21-type.

A(h)	$-0.0061h - 0.0017$
B(h)	$0.3025h^3 - 0.5728h^2 + 0.3929h - 0.0529$
C(h)	$0.0741h^3 - 0.1444h^2 + 0.1233h + 19.74$
A(w)	$-0.0084w^2 + 0.0667w + 0.0254$
B(w)	19.763